AJNR

This information is current as of July 31, 2025.

Carotid Body Detection on CT Angiography

R.P. Nguyen, L.M. Shah, E.P. Quigley, H.R. Harnsberger and R.H. Wiggins

R.P. Nguyen
L.M. Shah
E.P. Quigley
H.R. Harnsberger
R.H. Wiggins

Carotid Body Detection on CT Angiography

BACKGROUND AND PURPOSE: Advances in multidetector CT provide exquisite detail with improved delineation of the normal anatomic structures in the head and neck. The carotid body is 1 structure that is now routinely depicted with this new imaging technique. An understanding of the size range of the normal carotid body will allow the radiologist to distinguish patients with prominent normal carotid bodies from those who have a small carotid body paraganglioma.

MATERIALS AND METHODS: We performed a retrospective analysis of 180 CTAs to assess the imaging appearance of the normal carotid body in its expected anatomic location.

RESULTS: The carotid body was detected in >80% of carotid bifurcations. The normal size range measured from 1.1 to 3.9 mm ± 2 SDs, which is consistent with the reported values from anatomic dissections.

CONCLUSIONS: An ovoid avidly enhancing structure at the inferomedial aspect of the carotid bifurcation within the above range should be considered a normal carotid body. When the carotid body measures >6 mm, a small carotid body paraganglioma should be suspected and further evaluated.

ABBREVIATIONS: AP = anteroposterior; CTA = CT angiography

The carotid body is a structure usually located within the adventitia of the common carotid artery at the inferomedial aspect of the carotid bifurcation.[1] The carotid body has several functions in humans, including chemo- and baroreception and regulation of heart rate and blood pressure.[2] In anatomic dissections, the carotid body measures 5–7 mm in height and ranges in width from 2.5 to 4 mm.[3] To our knowledge, there is no reference in the imaging literature describing the normal cross-sectional appearance of the carotid body. In this article, we address the appearance of the normal carotid body on enhanced multidetector CT to provide a basis for distinguishing this structure from a small carotid body paraganglioma.

The most common pathology of the carotid body is the paraganglioma, a benign tumor that arises from glomus cells within this structure.[4] Glomus cells are part of the extra-adrenal neuroendocrine system located throughout the body, mostly in association with the autonomic nervous system. In the head and neck, these paraganglias migrate along a branchiomeric (of the branchial mesoderm) distribution and are found in distinct sites along the course of the carotid artery, aortic arch, and temporal bone. Mafee et al[4] noted that paraganglionic cells are also found less frequently in areas of the orbit (in association with the ciliary ganglion), pterygopalatine fossa (in association with the pterygopalatine ganglion), buccal mucosa, nasopharynx, and larynx. There is a normally progressive involution of the paraganglionic cells of these and other extra-adrenal locations. Paragangliomas of the head and neck have been classically categorized by location: at the carotid bifurcation, a carotid body tumor; 2 cm below skull base in the carotid space, a glomus vagale; at the jugular foramen, a glomus jugulare; and at the cochlear promontory, a glomus tympanicum.[5] There have been rare reports of paragangliomas in the oral cavity, thyroid gland, and larynx and along the facial nerve.[6-9]

Materials and Methods

Following institutional review board approval, a retrospective review was performed of 180 consecutive patients who underwent routine CTA of the neck during 1 year. Orthogonal measurements of the carotid body were performed bilaterally (Fig 1). From the initial patient population, 30 were randomly selected for repeat measurement to assess single intraobserver reliability of measurements. In addition to orthogonal measurements of the carotid body, regions of interest were placed over it and the corresponding internal carotid artery to evaluate any possible correlation of relative enhancement. The smallest axial region of interest measurable on our PACS workstation was used with an area of 0.0194 cm^2. The region of interest chosen as the carotid body was a reproducible ovoid avidly enhancing structure at the inferomedial aspect of the carotid bifurcation. This is the location of the carotid body as demonstrated by anatomists.[1,10] Tubular lesions suggesting vascular structures were not included because they did not correspond to the morphology of anatomically described carotid bodies. A retrospective chart review was then performed to collect data regarding patient age, sex, and smoking history.

The protocol for CTA of the cervical vasculature at our institution is standardized on all scanners. On all CT angiograms, we perform bolus tracking. Premonitoring scans are obtained at the level of the aortic arch with a region of interest placed within the ascending aorta. The helical acquisition of 0.6-mm collimated images is performed from the inferior aspect of the aortic arch to the superior aspect of the frontal sinus. Scans are acquired with a pitch of 0.8. The kilovoltage is set at 120 with a standard milliampere-second reference of 275. CARE Dose (Siemens Medical Solutions, Forchheim, Germany) is performed on all scans to minimize radiation, which results in variable milliampere-seconds. Contrast is injected through an 18-ga antecubital fossa intravenously with a volume of 100 mL at a rate of 4 mL/s. All scans are obtained with iopamidol contrast (Isovue 370; Bracco Diagnostics, Milan, Italy). Axial images are reconstructed with a B20 kernel algorithm at 1-mm thickness. Coronal and sagittal reconstruc-
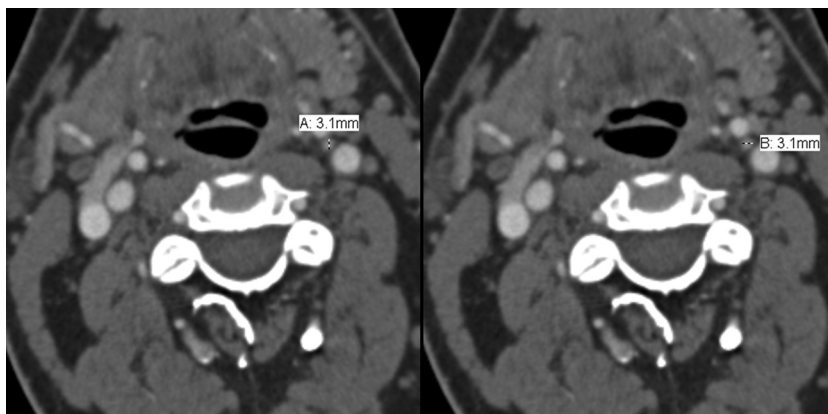
Fig 1. Representative axial CTA images demonstrate the method of orthogonal measurements, which were performed bilaterally.

Fig 2. Oblique sagittal reformations were performed with a B20 kernel at a 2-mm thickness and at 2-mm increments. The normal carotid body is seen at the carotid bifurcation.

Fig 3. Bar graph shows the distribution in size of the carotid body based on measurements of 358 carotid bodies. The right carotid body measures an average of 2.4 (transverse) × 2.0 (AP) ± 0.8 (transverse) and 0.6 (AP) mm. The left carotid body measures, on average, 2.2 (transverse) × 2.1 (AP) ± 0.7 (transverse) and 0.5 (AP) mm. The range of normal defined as 2 SDs is 1.1–3.9 mm for the carotid body.
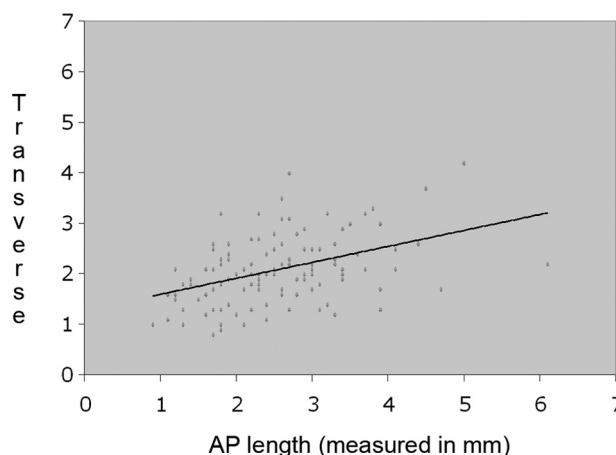
Fig 4. Line graph shows that the Pearson coefficient of the transverse dimension of the right carotid body to the left is 0.52 with a *P* value of <.0001. The data indicate a correlation between the AP and transverse dimensions of the right and left carotid bodies.
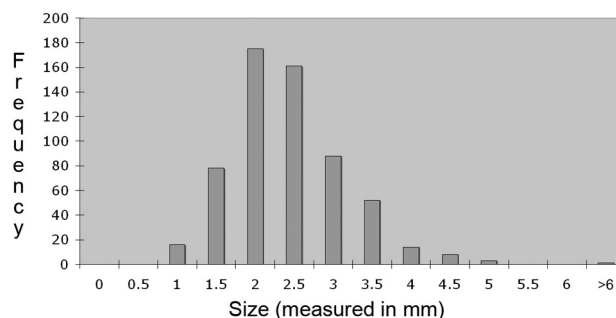
tions are performed with a B20 kernel algorithm at 2-mm thickness and at 2-mm increments (Fig 2).

All measurements were performed by using a standardized protocol on PACS with 200% magnification. All studies were viewed at the same window/level settings and the same hanging protocol.

Results

There were a total of 180 CTAs initially evaluated. One patient was excluded from the study due to the presence of a carotid body tumor. The normal carotid body could be seen on most scans. The right carotid body was seen on 82.6% of CTAs (148 of 179 studies). The left carotid body was seen on 86.0% of scans (154 of 179 studies). The right carotid body measured an average of 2.4 mm in the transverse dimension and 2.0 in the AP dimension. The SDs were 0.8 mm for the transverse dimension and 0.6 mm for the AP dimension. The left carotid body measured, on average, 2.2 mm in the transverse dimension and 2.1 mm in the AP dimension. The SDs for the transverse and AP measurements were 0.7 mm and 0.5 mm, respectively. The average Hounsfield unit for the carotid body was 135 ± 46, and for the internal carotid artery, 399 ± 100.

The initial protocol design was to measure the carotid body in 3 orthogonal planes. However, the helical CT protocol reconstruction limits accurate measurement in the craniocaudal plane below 2 mm. Due to this craniocaudal limitation, the protocol was modified to measure the carotid body in the axial plane only. The range of normal, defined as 2 SDs, was 1.1–3.9 mm for the carotid body (Fig 3).

With the Pearson correlation coefficient, the size of the right carotid body was highly correlated with the size of the left. The Pearson coefficient of the transverse dimension of the right carotid body to the left was 0.52 with a *P* value of <.0001 (Fig 4). In the AP dimension, the Pearson coefficient between sides was 0.43 with a *P* value of <.0001 (Fig 5).

Reliability testing and intraclass correlation statistical analysis were performed on a group of 30 randomly selected patients to evaluate intraobserver reproducibility of measure-
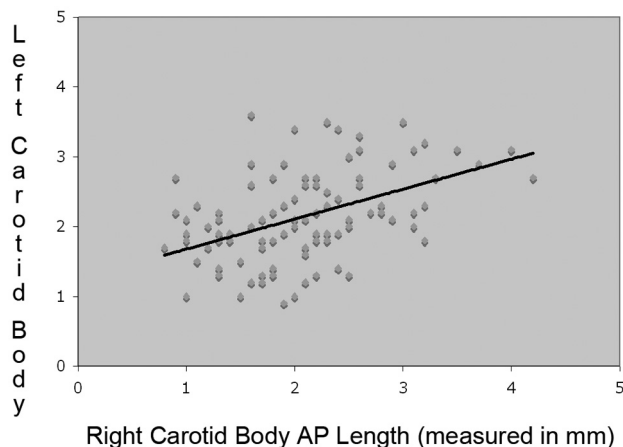
Fig 5. Line graph shows that the Pearson coefficient of the AP dimension of the right carotid body to the left is 0.43 with a P value of <.0001. This illustrates a correlation between the size of the right and left carotid bodies.

Fig 6. Axial CTA image depicts an avidly enhancing mass at the right carotid bifurcation splaying the internal (white arrow) and external carotid arteries (black arrows). There are numerous central and peripheral enlarged feeding arterial branches within this carotid body tumor.

ments. All examinations were de-identified for measurement, and the interpreting neuroradiologist was blinded to any identifiers. The 30 selected patients were mixed into the study population with identical duplicated examinations to obtain 3 separate measurements in the selected population to evaluate intraobserver reproducibility. The intraclass correlation coefficient for the right and left sides ranged between 0.94 and 1.0.

Analysis of covariance with age, sex, and smoking as predictor variables for size was also performed. These analyses did not demonstrate any statistical significance. In addition, the degree of enhancement of the carotid body did not correlate with the size of the carotid body or the degree of enhancement of the ipsilateral internal carotid artery.

Discussion

The carotid body is located at the inferomedial aspect of the carotid bifurcation. All paraganglia are composed of chief cells (type I cells; ie, chemoreceptive cells) and sustentacular cells (type II cells; ie, supporting cells). The specific ratio of the 2 types of cells determines the function of that particular paraganglion. Developmentally, both types of cells are of neuroectodermal origin, arising from neural crest cells.[11] The glomus type I cells release a variety of neurotransmitters, including acetylcholine, adenosine triphosphate, and dopamine, which trigger excitatory postsynaptic potentials in synapsed neurons leading to the respiratory center. The glomus type II cells resemble glia, express the glial marker S100, and act as supporting cells. Furthermore, these supporting cells appear to behave as stem cell precursors for glomus type I cells under chronic hypoxic conditions.[12] The histopathology of carotid body tumors shows nests of polygonal chief cells (zellballen) enclosed by trabeculae of fibrous and sustentacular elongated cells.[5,13]

The carotid body is a highly vascular structure. Barnett et al[14] used radioactive microspheres to demonstrate that blood flow to the carotid body was highest compared with several other organs studied. This high vascularity is essential to the function of the carotid body for detecting changes in the composition of blood in the common carotid artery because it forms the internal and external carotid arteries.[15] The predominant function is the detection of the partial pressure of oxygen, but it is also sensitive to the partial pressure of CO_2
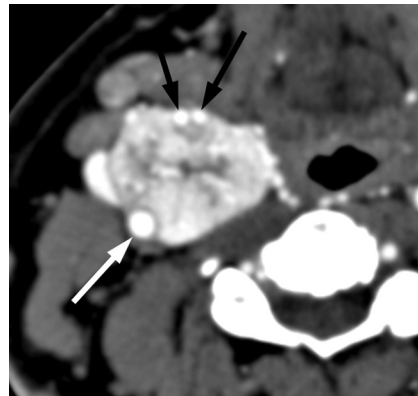
and pH and temperature.[12] The carotid body sends feedback to the cardiorespiratory centers in the medulla oblongata via the afferent branches of the glossopharyngeal nerve, whose cell bodies are located in the petrosal ganglion. The afferent fibers of the aortic body chemoreceptors are relayed by the vagus nerve. These centers regulate breathing and blood pressure.[16] Glomus cells are also activated by hypoglycemia.[17] It is, however, the sensitivity to acute changes of O_2 tension that makes the carotid body fundamental for the adaptive hyperventilatory reflex in response to hypoxemia.[16]

A carotid body paraganglioma (carotid body tumor) is a rare tumor. The glomus bodies are subdivided into classes on the basis of their location. The carotid body tumor is named for the glomus body of origin and its characteristic location at the bifurcation of the common carotid artery. These tumors have both genetic and environmental risk factors. Populations living at higher elevations or in a chronic hypoxic state are thought to have a higher incidence of paragangliomas.[18-20] The clinical prognosis of carotid body tumors is usually favorable due to their location and relative accessibility for surgical resection.[21] However, surgery can be challenging because the tumor is highly vascular and often densely adherent to the carotid bifurcation with intimate association of cranial nerves X and XII. The surgical grouping of Shamblin et al[22] is based on the relationship of the tumor with the carotid vessels, which establishes the risk of surgical intervention and is a predictor of vascular morbidity.

These tumors are easily visualized with current CT and MR imaging modalities. On imaging, a carotid body tumor typically presents as an avidly enhancing soft-tissue mass at the carotid bifurcation (Fig 6). Larger carotid body tumors have a typical imaging appearance, including avid enhancement, splaying the carotid bifurcations, and the characteristic "salt and pepper" appearance on T1-weighted MR imaging due to slowly flowing blood products and vascular flow voids.

Small lesions in the carotid bifurcation present a challenging diagnostic dilemma to the radiologist. A prominent normal carotid body must be considered against a small carotid body paraganglioma, nerve sheath tumor, or sympathetic chain schwannoma. Given that the normal carotid body is now routinely seen on multidetector CTA studies (Fig 7), an objective understanding of its normal acceptable size range is
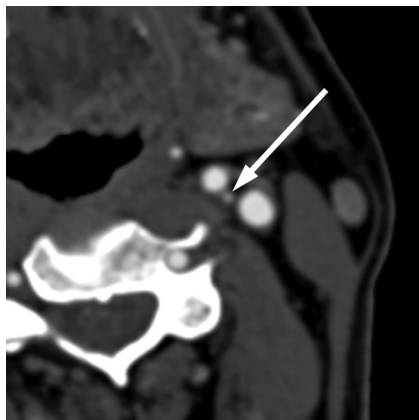
Fig 7. Axial CTA exhibits a small enhancing structure at the left carotid bifurcation, corresponding to a normal carotid body.

Conclusions

This study demonstrates the importance of recognizing the normal carotid body, which can now be seen routinely on CTAs of the neck. The carotid body is an enhancing soft-tissue mass at the carotid bifurcation with transverse and AP imaging dimensions ranging from 1.1 to 3.9 mm $\pm$ 2 SDs. These values are consistent with reported anatomic dissections.[2] Due to volume averaging, the minimum section thickness required to visualize the carotid body is 1 mm. One should expect to see an ovoid avidly enhancing structure at the inferomedial aspect of the carotid bifurcation within this size range in a majority of thin-section contrast-enhanced CT studies, and it should not raise concern. Further imaging or interventions, which are associated with higher cost and patient morbidity, are not needed. Lesions measuring >6 mm (>2 SDs) raise concern for small paragangliomas of the carotid body, especially in those individuals with a family history of paragangliomas, and require further investigation.

critical. Diagnosing a prominent-appearing but normal carotid body as a small carotid body paraganglioma must be avoided to prevent unnecessary surgical intervention.

While development of a carotid body tumor is associated with genetic and environmental risks, there appears to be no such association with the size of the normal carotid body. We hypothesized that the size of the carotid body would be larger in patients with a smoking history or living at high altitudes. However, this association was not the case in our series. Additionally, we postulated that the size of the carotid body would vary with sex. This also did not prove to be correct.

Finally, the carotid body is a chemo- and baroreceptor located in the adventitia of the carotid bifurcation. We hypothesized that the degree of enhancement of the carotid body would be correlated with the degree of contrast flowing through the ipsilateral carotid artery. This final hypothesis also proved false. There was no correlation of enhancement in the carotid body and the adjacent artery. Furthermore, we found a wide variance in the degree of enhancement of the carotid body and the adjacent artery. This is likely related to the degree of variation in the arrangement of the carotid bifurcation because the carotid body draws its blood from arteries originating from this area. Studies have shown a lack of uniformity of the vascular pattern in animals of different species and in animals of the same species.[23] Statistical analysis of the degree of enhancement of the carotid body in relation to variables such as sex, age, and smoking history did not show a significant correlation. However, the variability in enhancement should not deter one from confidently measuring the enhancing ovoid structure at the inferomedial aspect of the carotid bifurcation as the carotid body.

A limitation of our study is the linear method of measurement. A volumetric measurement, we thought, would be of questionable accuracy because most of the carotid bodies have a variable oval-to-round shape in the axial plane and, even then, are not symmetric. To our knowledge, there is no imaging correlate published to date describing the linear method of measurement, and the published anatomic descriptions are volumetric, weight-based, or linear in terms of their measurements of the carotid body. Cadaveric correlation was pursued but was not feasible due to the fragile macerated state of the carotid body tissue with dissection attempts.

References

1. Lack EE. **Tumors of the adrenal gland and extra-adrenal paraganglia.** Rosai J, eds. *Atlas of Tumor Pathology.* Washington, DC: Armed Forces Institute of Pathology; 1997:303–409
2. Kliewer KE, Cochran AJ. **A review of the histology, ultrastructure, immuno-histology, and molecular biology of extra-adrenal paragangliomas.** *Arch Pathol Lab Med* 1989;113:1209–18
3. Standring S. *Grey's Anatomy.* 39th ed. New York: Elsevier; 2005:547
4. Mafee MF, Raofi B, Kumar A, et al. **Glomus faciale, glomus jugulare, glomus tympanicum, glomus vagale, carotid body tumors, and simulating lesions: role of MR imaging.** *Radiol Clin North Am* 2000;38:1059–76
5. Rao AB, Koeller KK, Adair CF. **From the archives of the AFIP: paragangliomas of the head and neck—radiologic-pathologic correlation. Armed Forces Institute of Pathology.** *Radiographics* 1999;19:1605–32
6. Boros AL, Davis JP, Sedghizadeh PP, et al. **Glomus tumor: report of a rare case affecting the oral cavity and review of the literature.** *J Oral Maxillofac Surg* 2010;68:2329–34
7. Ferri E, Manconi R, Armato E, et al. **Primary paraganglioma of thyroid gland: a clinicopathologic and immunohistochemical study with review of the literature.** *Acta Otorhinolaryngol Ital* 2009;29:97–102
8. Marlowe SD, Swartz JD, Koenigsberg R, et al. **Metastatic hypernephroma to the larynx: an unusual presentation.** *Neuroradiology* 1993;35:242–43
9. Petrus LV, Lo WM. **Primary paraganglioma of the facial nerve canal.** *AJNR Am J Neuroradiol* 1996;17:171–74
10. Molenda O. **Morphology and topography of the carotid body and carotid sinus in sheep (Ovis ammon f. aries L., 1758)** [in Polish]. *Pol Arch Weter* 1975;18:343–64
11. Gonzalez C, Almaraz L, Obeso A, et al. **Carotid body chemoreceptors: from natural stimuli to sensory discharges.** *Physiol Rev* 1994;74:829–98
12. Fitzgerald RS, Eyzaguirre C, Zapata P. **Fifty years of progress in carotid body physiology–invited article.** *Adv Exp Med Biol* 2009;648:19–28
13. Wieneke J, Smith A. **Paraganglioma: carotid body tumor.** *Head Neck Pathol* 2009;3:303–06
14. Barnett S, Mulligan E, Wagerle LC, et al. **Measurement of carotid body blood flow in cats by use of radioactive microspheres.** *J Appl Physiol* 1988;65:2484–89
15. O'Regan RG, Majcherczyk S. **Role of peripheral chemoreceptors and central chemosensitivity in the regulation of respiration and circulation.** *J Exp Biol* 1982;100:23–40
16. López-Barneo J, Ortega-Sáenz P, Pardal R, et al. **Carotid body oxygen sensing.** *Eur Respir J* 2008;32:1386–98
17. Pardal R, López-Barneo J. **Low glucose-sensing cells in the carotid body.** *Nature Neurosci* 2002;5:197–98
18. Pacheco-Ojeda L, Durango E, Rodriquez C, et al. **Carotid body tumors at high altitudes: Quito, Ecuador.** *World J Surg* 1988;12:856–60
19. Arias-Stella J, Valcarcel J. **Chief cell hyperplasia in the human carotid body at high altitudes: physiologic and pathologic significance.** *Hum Pathol* 1976;7:361–73
20. Heath D, Edwards C, Harris P. **Post-mortem size and structure of the human carotid body: its relation to pulmonary disease and cardiac hypertrophy.** *Thorax* 1970;25:129–40
21. Unlu Y, Becit N, Ceviz M, et al. **Management of carotid body tumors and familial paragangliomas: review of 30 years' experience.** *Ann Vasc Surg* 2009;23:616–20
22. Shamblin WR, ReMine WH, Sheps SG, et al. **Carotid body tumor (chemodectoma): clinicopathologic analysis of ninety cases.** *Am J Surg* 1971;122:732–39
23. Chungcharoen D, De Burgh Daly M, Schweitzer A. **The blood supply of the carotid body in cats, dogs and rabbits.** *J Physiol* 1952;117:347–58